FEEDBACK OPTIMIZATION OF GRID OSCILLATORS

Wayne A. Shiroma[1] and Zoya B. Popović[2]

[1] Department of Electrical Engineering, University of Hawaii at Manoa, Honolulu, HI, 96822, USA
[2] Department of Electrical and Computer Engineering, University of Colorado, Boulder, CO, 80309, USA

Abstract— **We present a method for optimizing the feedback level in a transistor-grid oscillator. Based on the approximate large-signal S-parameters of the transistor, an equivalent circuit model for the grid is synthesized for maximum oscillator power. The resulting circuit serves as a convenient benchmark for determining the level of feedback for a given grid. Experimental results demonstrate how the substrate thickness and metallization pattern affect power performance. A grid with an asymmetric unit cell is shown to deliver almost 60% more effective radiated power than a grid with a symmetric unit cell.**

I. Introduction

Grid oscillators are large-scale power combiners that have shown promise for realizing moderate to high-power millimeter-wave sources [1]. Designing a grid oscillator first of all requires that the steady-state oscillation condition [2] be met. In addition, for a power-grid design, the load resistance must be optimized and the feedback level adjusted so that the device operates at maximum power-added efficiency [3]. To meet all of these constraints simultaneously at the desired oscillation frequency, the grid dimensions, substrate parameters, external tuners, and metallization pattern must be adjusted iteratively. Even with the aid of equivalent circuit models, this process can be quite tedious and time-consuming.

This paper presents a technique for optimizing the feedback level and power output of a grid oscillator. Section II explains how the circular function [4] describes saturation effects in an oscillator, and suggests that an optimal circular function exists for achieving maximum oscillator power. It also discusses how a grid can be reduced to an equivalent two-port embedding circuit and how this circuit can be synthesized to maximize oscillator power. In Section III, the optimum circular function is used as a benchmark for assessing the performance of several experimental grids.

II. Method

A. Linear Oscillator Analysis

A grid oscillator is a quasi-optical implementation of a two-port feedback oscillator, where one network represents the transistor and the other represents the embedding circuit, which includes the grid metallization,

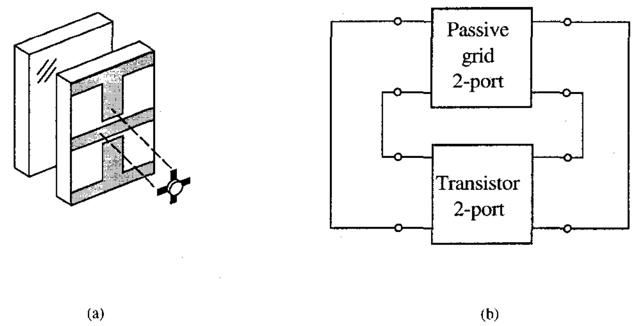

Fig. 1. (a) Unit cell of a grid oscillator with the transistor and passive grid separated. (b) Feedback-oscillator model consisting of the embedding network and the transistor model.

dielectric substrate, mirror, and free space (Fig. 1). The latter network is obtained from a full-wave analysis as described in [5]. One way of determining whether the circuit oscillates is to compute its circular function [4], given by

$$C = \frac{S_{11}S'_{11} + S_{21}S'_{12} - |\mathbf{S}||\mathbf{S}'|}{1 - S_{12}S'_{21} - S_{22}S'_{22}}, \tag{1}$$

where S_{ij} and S'_{ij} are the S-parameters of the transistor and feedback network, respectively. If (1) is evaluated using the transistor's small-signal S-parameters, oscillation start-up requires that $|C| > 1$. To reach steady state, gain saturation causes the transistor S-parameters to change until the condition $C = 1\angle 0°$ is satisfied at the oscillation frequency. Equation (1) then becomes a special case of the generalized oscillation condition [2] for an n-port feedback oscillator where $n = 2$.

Fig. 2 illustrates the circular-function analysis of two grid oscillators with identical unit cells, but different dielectric and mirror characteristics. Fig. 2(a) shows the circular function for the transistor-loaded grid in free space, with no dielectric substrate or mirror. Since the magnitude of the circular function is less than one, no oscillation is possible. However, when the grid is backed by a 6.35-mm-thick substrate with $\epsilon_r = 10.2$, two modes are predicted, at 2.8 and 6.5 GHz (Fig. 2(b)). This agrees with measured oscillation modes at 2.7 and 6.4 GHz. Each mode was obtained separately at different DC bias currents: 5 mA/device for the 2.7-GHz mode and 12 mA/device for the 6.4-GHz mode.

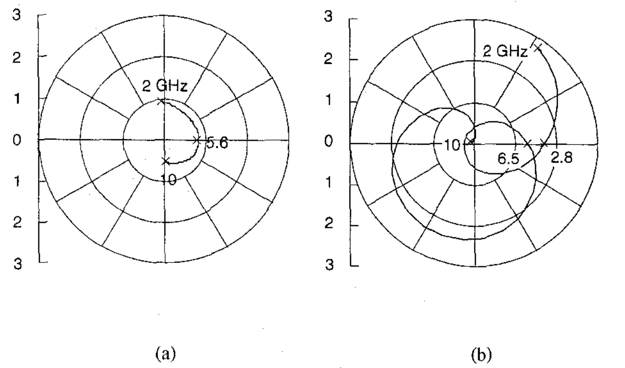

Fig. 2. Circular functions for a transistor-loaded grid (a) in free space, with no substrate or mirror, and (b) backed by a thick, high-permittivity substrate and mirror. The active device is an HP-Avantek ATF-26836 General Purpose MESFET. Small-signal S-parameters (for $V_{ds} = 3\,\text{V}$, $I_{ds} = 10\,\text{mA}$) supplied by the manufacturer are used in the simulation.

B. Quasi-Linear Oscillator Analysis

The linear analysis above is based on the small-signal transistor S-parameters. To properly include the effect of gain saturation, which is necessary in actual oscillator operation, a nonlinear analysis is required. If a nonlinear model of the transistor is unavailable, a quasi-linear analysis can serve as an approximation [6].

In this case, it is useful to use the concept of maximum-efficient gain [7], [8], defined as

$$G_{\text{ME}} = \frac{|S_{21}/S_{12}|^2 - 1}{2\,(K|S_{21}/S_{12}| - 1)}, \tag{2}$$

where

$$K = \frac{1 + |S_{11}S_{22} - S_{21}S_{12}|^2 - |S_{11}|^2 - |S_{22}|^2}{2|S_{12}||S_{21}|}.$$

Johnson [6] showed that the large-signal value of G_{ME} corresponding to maximum oscillator power is

$$G_{\text{ME,opt}} = \frac{G_{\text{ME,ss}} - 1}{\ln G_{\text{ME,ss}}}, \tag{3}$$

where $G_{\text{ME,ss}}$ is the value of (2) computed using the small-signal transistor S-parameters. The gain compression corresponding to the optimum operating point is then

$$GC_{\text{opt}} = G_{\text{ME,ss}} - G_{\text{ME,opt}}. \tag{4}$$

Since the S-parameters are frequency-dependent, the circular function is actually a locus of points, but the particular point of interest for this discussion is the frequency at which $\angle C = 0°$. Two cases are shown in Fig. 3.

In the optimum case, the small-signal value of C should be displaced from its large-signal, steady-state value (*i.e.*, $1\angle 0°$) by an amount corresponding to GC_{opt} (Fig. 3(a)). Since this value of C corresponds to the optimum case, it is referred to as C_{opt}. There are two operating points shown in Fig. 3(b) that represent suboptimal performance. Both cases have less than the maximum available oscillator power, but for different reasons: point A suffers from gain compression that is too low ($GC_{\text{A}} < GC_{\text{opt}}$), while point B suffers from gain compression that is too high ($GC_{\text{A}} > GC_{\text{opt}}$). For point A, the transistor operates in the near-linear regime since the circular function requires only a small amount of gain compression to reach steady state. For point B, the transistor is heavily saturated since the feedback level is too high.

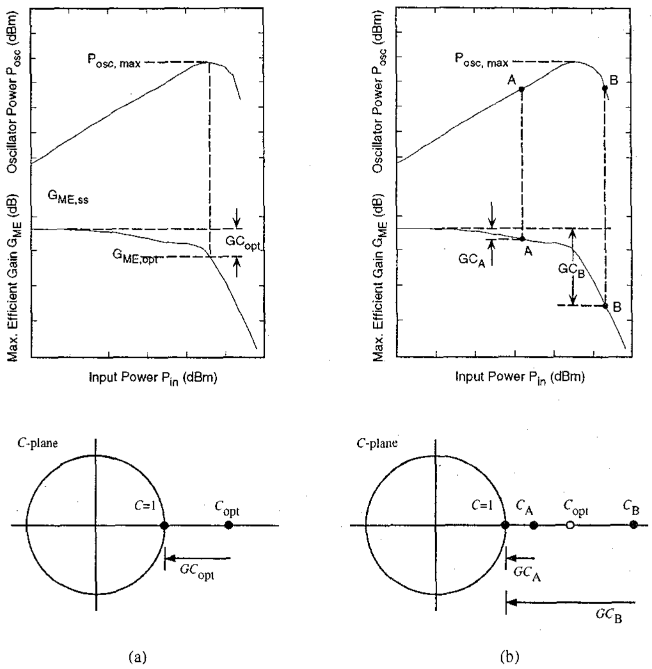

Fig. 3. Transistor saturation characteristics and circular-function plane for (a) the optimal operating point, and (b) two suboptimal operating points.

There are several disadvantages of operating at point B. In the over-saturated regime, the oscillator power drops off more sharply, so it is more sensitive to design variations in the feedback network. An oscillator operating in the nonlinear regime is also more likely to have higher harmonic content. For a MESFET, point B is also associated with high input power at the gate, which could cause the Schottky gate diode to be driven into forward-bias; this could result in a large current density in the gate metallization which can lead to degraded device reliability.

Unfortunately, most grid oscillators demonstrated to date have had too much feedback [3]. The design of

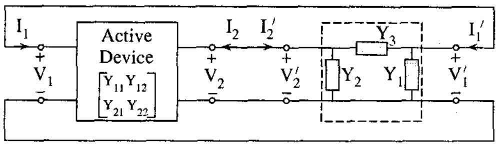

Fig. 4. A feedback oscillator consisting of an active device with known Y-parameters and an embedding network with unknown circuit elements. The embedding circuit is assumed to have a Π topology.

an optimized grid must therefore include a feedback-reduction mechanism to move the circular function toward C_{opt}. To calculate C_{opt} from (1) requires knowing the S-parameters of both the transistor and the optimum feedback network. The general approach to optimizing the feedback network of an oscillator is described in [9]. In short, an equivalent Π network as shown in Fig. 4 is synthesized which satisfies the oscillation condition and sets the proper feedback level and load resistance for maximum power. For grids, the equivalent Π network is composed of purely reactive elements in the shunt legs (Y_1 and Y_2) and a resistive-reactive combination in the series arm (Y_3). Explicit expressions for the circuit elements are derived in [10]. Once the optimum embedding network has been derived for a given transistor, C_{opt} can be computed from (1) and used as a benchmark for determining whether a given grid oscillator is over- or under-compressed.

III. Experimental Results

In this section, experimental results for several grids are presented to demonstrate how the grid feedback affects output power.

A. C-Band pHEMT Grid Oscillator

The first example is a 5×5 pHEMT grid oscillator with varying substrate thickness. Three C-functions, corresponding to three different thicknesses, are shown in Fig. 5.

Since the oscillation frequency is different for each case (see Table I), three different optimum embedding circuits can be derived. The one for 5 GHz is shown in Fig. 6. The 1.10 pF and 0.56 pF capacitors represent the gate-source and drain-source gaps of the grid, respectively. The inductor and resistor model the lead inductance, load resistance, substrate, and mirror characteristics. The optimum C-function is found from (1), using the S-parameters for this circuit as well as those of the pHEMT. For the three different frequencies, C_{opt} is plotted in Fig. 5.

Since $|C| > |C_{\text{opt}}|$ for all three cases, we immediately conclude that the grids are over-compressed. Moreover, the grid with the thinnest substrate is the most compressed, and should have the least power. The experimental results in Table I support this. The existence of harmonics also supports the view that these oscillators are over-compressed.

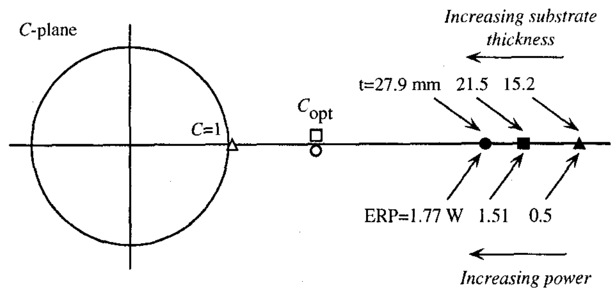

Fig. 5. Operating points corresponding to three different substrate thicknesses for a C-band pHEMT grid oscillator. The shaded symbols represent the C-functions of the grids, and the open symbols represent the C-functions of the theoretical optimum networks.

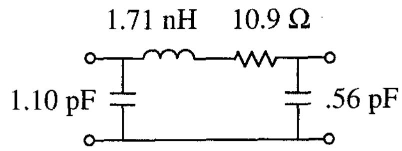

Fig. 6. Optimum embedding circuit for the HP ATF-35576 pHEMT at 5 GHz.

B. X-Band MESFET Grid Oscillators

The example above demonstrates how the feedback level can be controlled by varying the substrate thickness. Another way of controlling the feedback is to alter the unit-cell geometry in some way. Hacker [3] used a meandered gate lead to control the compression level in a gate-feedback grid. For a source-feedback grid, the feedback can be controlled by using an asymmetric unit cell (Fig. 7(a)), as suggested by the asymmetric optimum circuit of Fig. 6. The drain is connected to a short dipole radiating element, as before. However, the width of the radiating element connected to the gate is extended across the full width of the unit cell, resulting in a slot, rather than dipole radiator. By adjusting the dimensions of this slot, the amount of feedback to the gate, and hence the compression level, can be controlled to some extent.

TABLE I

C-Band pHEMT Grid Oscillator

Substrate Thickness (mm)	Osc. Freq. (GHz) Sim.	Meas.	% Err.	Meas. ERP (W)	Harmonics(dBc) 2^{nd}	3^{rd}
15.2	6.4	6.07	5	0.50	-28	-42
21.5	4.6	4.86	5	1.51	-25	-45
27.9	5.1	5.32	4	1.77	-31	-45

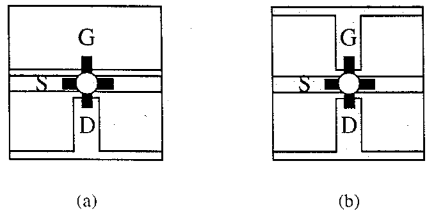

Fig. 7. Unit cell of a grid oscillator with (a) slot/dipole radiating elements and (b) dipole radiating elements. Both cells are 6 mm square and are loaded with HP ATF-26884 MESFETs. The grids are printed on a 0.5-mm substrate (*Duroid* 5880, $\epsilon_r = 2.2$) and placed on a second 5-mm layer (*Duroid* 6010.8, $\epsilon_r = 10.8$) which is metallized on the back.

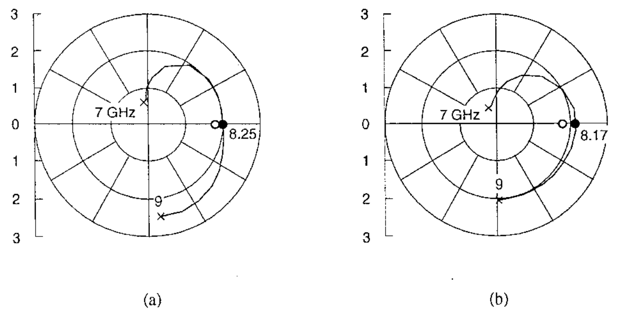

Fig. 8. C-functions for the (a) slot/dipole and (b) dipole grid oscillators. The shaded symbols represent the C-functions of the grids, and the open symbols represent the C-functions of the theoretical optimum networks.

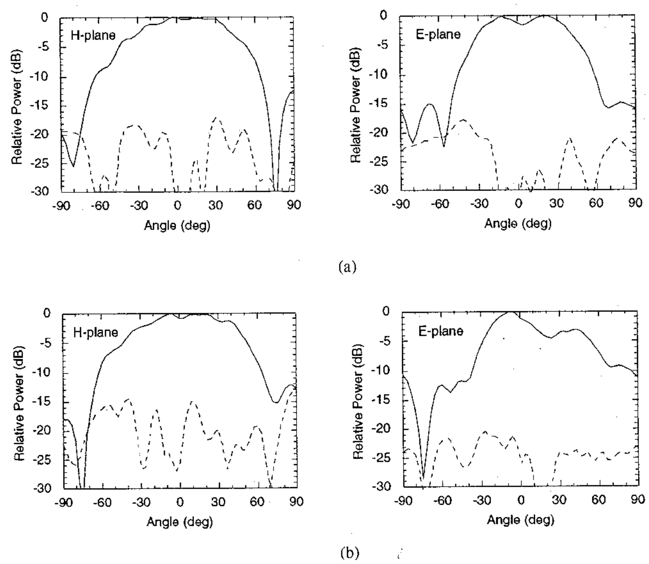

Fig. 9. Measured H- and E-plane patterns of the (a) dipole/slot and (b) dipole grid oscillators of Fig. 7. Solid lines represent the co-polarization and dashed lines represent the cross-polarization.

TABLE II

X-Band MESFET Grid Oscillator

Unit-Cell Geometry	Osc. Freq. (GHz) Sim.	Meas.	% Error	Meas. ERP (W) $V_{ds} = 3$ V	$V_{ds} = 4$ V
Slot/Dipole	8.3	8.57	3	0.31	0.49
Dipole	8.1	8.35	3	0.19	0.31

To demonstrate, two 4×4 X-band grid oscillators were fabricated with the metallization patterns shown in Fig. 7. Both grids have the same unit-cell dimensions, substrate, and mirror spacing. The simulated C-functions are shown in Fig. 8. At the same DC bias level, the slot/dipole-grid oscillator demonstrated up to 58% more ERP than the dipole-grid oscillator (Table II). While both grids are slightly over-compressed, they are not as compressed as the pHEMT grids discussed earlier. No harmonics were observed for either grid.

Fig. 9 shows the measured radiation patterns. Based on an estimate of the directivity from these patterns, the highest conversion efficiency for the slot/dipole grid was 21%, while that of the dipole grid was about 10%.

Acknowledgments

This work was supported in part by the US Army Research Office under Contract #DAAL03-92-G-0265 and the AASERT Program, and in part by the National Science Foundation under a Presidential Faculty Fellow Award.

References

[1] Z. B. Popović, R. M. Weikle II, M. Kim, and D. B. Rutledge, "A 100-MESFET planar grid oscillator," *IEEE Trans. Microwave Theory Tech.*, vol. 39, pp. 193–200, Feb. 1991.

[2] A. P. S. Khanna and J. Obregon, "Microwave oscillator analysis," *IEEE Trans. Microwave Theory Tech.*, vol. MTT-29, pp. 606–607, June 1981.

[3] J. B. Hacker, M. P. DeLisio, M. Kim, C.-M. Liu, S.-J. Li, S. W. Wedge, and D. B. Rutledge, "A 10-Watt X-band grid oscillator," in *1994 IEEE MTT-S Int. Microwave Symp. Dig.*, (San Diego, CA), pp. 823–826, May 1994.

[4] R. D. Martinez and R. C. Compton, "A general approach for the s-parameter design of oscillators with 1 and 2-port active devices," *IEEE Trans. Microwave Theory Tech.*, vol. 40, pp. 569–574, Mar. 1992.

[5] S. C. Bundy and Z. B. Popović, "A generalized analysis for grid oscillator design," *IEEE Trans. Microwave Theory Tech.*, vol. 42, pp. 2486–2491, Dec. 1994.

[6] K. M. Johnson, "Large signal GaAs MESFET oscillator design," *IEEE Trans. Microwave Theory Tech.*, vol. MTT-27, pp. 217–227, Mar. 1979.

[7] K. L. Kotzebue, "Maximally efficient gain: A figure of merit for linear active 2-ports," *Electronics Lett.*, vol. 12, pp. 490–491, 16th Sept. 1976.

[8] K. L. Kotzebue, "Microwave amplifier design with potentially unstable FET's," *IEEE Trans. Microwave Theory Tech.*, vol. MTT-27, pp. 1–3, Jan. 1979.

[9] M. Vehovec, L. Houselander, and R. Spence, "On oscillator design for maximum power," *IEEE Trans. Circuit Theory*, vol. CT-15, pp. 281–283, Sept. 1968.

[10] K. L. Kotzebue and W. J. Parrish, "The use of large-signal S-parameters in microwave oscillator design," in *Proc. 1975 Int. Microwave Symp. on Circuits and Systems*, 1975.